



Investigation of ammonium acetate effect on electroless Ni-P deposits

A. Elhaloui^{1,2}, T. Anik¹, M. Ebn Touhami¹, A. Shaim¹, K. Iyach³,
R. Touri¹, M. Sfaira², M. Mcharfi², B. Hammouti⁴

¹Laboratoire des Matériaux, d'Electrochimie et d'Environnement, Faculté des Sciences, Université Ibn Tofaïl, BP. 133 – 14000, Kénitra, Morocco.

²Laboratoire d'Ingénierie des Matériaux, de Modélisation et d'Environnement, LIMME, Faculté des Sciences Dhar El Mahraz, Université Sidi Mohammed Ben Abdellah, USMBA, BP 1796 – 30000, Atlas – Fès, Morocco.

³Académie des Arts Traditionnels – Fondation Mosquée Hassan II – Hassan II.

⁴LCAE-URAC18, Faculté des Sciences, Université Mohammed Premier, BP 717 – 60000, Oujda, Morocco.

Received 21 Jan 2015, Accepted 15 Apr 2015, Accepted 15 Apr 2015

*Corresponding authors: Pr. M. EbnTouhami, Tel: +212 6 6158 63 00; E-mail address: mebntouhami@yahoo.fr

Abstract

The effect of ammonium acetate on the formation and characteristics of Ni-P electroless deposition obtained from an acidic medium using sodium hypophosphite such as reducing agent was investigated. The obtained results showed that the deposition rate, the surfaces morphology, the crystalline structure and the roughness of deposit depend on the ammonium acetate concentration. In addition, it is noted that the increase of ammonium acetate caused a change in phosphorus content of the deposits. Indeed, the kinetics studies of electroless Ni-P deposits were investigated using cyclic voltammetry and electrochemical impedance spectroscopy measurements. It is found that these kinetics parameters of electroless Ni-P deposits depend also on the ammonium acetate concentration.

Keywords : Electroless deposition of Ni-P; Ammonium acetate effect; Surfaces morphology; RXD analysis; Kinetics studies; EIS studies.

Introduction

Electroless nickel process is undoubtedly the most important catalytic plating process in use today to solve materials problem in various industries. Its steadily increasing use can be attributed to marked improvements in solution stability and the equipment used, however, during several decades, the electroless nickel bath could decompose spontaneously during the deposition process. This decomposition was generally preceded by an increase in the volume of hydrogen gas evolved [1] and the precipitation of nickel phosphide [2, 3]. So, stabilizers are added to retard or prevent the onset of the homogeneous reaction which causes the subsequent random decomposition of the plating bath [4, 5] and the actual constituents of an EN solution include a Ni(II) salt, a reducing agent, suitable metal coordination ligands, stabilizers, and additives for particular needs.

The additives present in EN baths like stabilizers, complexing, accelerators and buffers influence kinetics and mechanism of the crystal growth process, bath passivation process, structure and morphology of the deposit, physical properties and purity of the deposit [6, 7]. They act on the deposition rate, the bath stability, the deposition quality and the corrosion resistance. Indeed, the ammonium acetic is selected as the main complexing agent in the nickel electroless deposition [8]. Also, $(\text{CH}_2)_2(\text{COOH})_2$, $(\text{NH}_4)_2\text{SO}_4$, NaF, CH_3COONa , H_3BO_3 , and

NH₄F are added to the bath as the buffering agents [7]. In other studies, thiourea and lead acetate are commonly employed as stabilizers in electroless plating baths [9, 10]. Complexing agents as lactates, hydroxy-acetate, glycines, malonates and certain fluorites [11] can be added. In addition, some heterocyclic organic compounds, such as mercaptobenzothiazole (MBT), are widely used as accelerators in electroless plating processes [12]. The ammonium fluoride [7], thiourea and succinic acid have also been found to exhibit an accelerating effect [13]. The action of these different compounds added to stabilize the EN bath or to accelerate the deposition rate depend on several parameters such as their concentration, pH, temperature, solution fluid dynamics, reducing agents and the presence of foreign species [14].

This paper presents the influence of ammonium acetate concentration in EN bath on the deposition rate, composition, morphology and structure of Ni-P coatings. In addition, we have investigated the deposition kinetics using cyclic voltammetry and electrochemical impedance spectroscopy.

2. Experimental procedures

All solutions employed these experiments were freshly prepared from analytical grade reagents and distilled water. The EN bath composition and operating conditions are listed in Table 1.

Table 1 : Baths compositions and operating conditions of Ni-P electroless deposition.

| Bath composition and operating conditions | Values |
|--|----------------|
| NiSO ₄ ; 6 H ₂ O (g L ⁻¹) | 30 |
| NaH ₂ PO ₂ ; H ₂ O (g L ⁻¹) | 23 |
| Na ₃ C ₆ H ₅ O ₇ ; 2 H ₂ O (g L ⁻¹) | 10.5 |
| CH ₃ COONH ₄ (g L ⁻¹) | From 0 to 32.5 |
| pH | 5.50 ± 0.01 |
| T (°C) | 85 ± 2 |

This bath contained nickel sulfate as a nickel ion source, sodium hypophosphite as a reducing agent, sodium citrate as a complexing agent, and ammonium acetate as an additive. The pH was fixed at 5.50 ± 0.01 with acetic acid addition and the temperature was held at 85 ± 2 °C.

The electrolysis cell was a borosilicate glass (Pyrex[®]) cylinder closed by cap with five apertures. Iron foil (or plate), 12 cm²/L active surface, was used as the substrate. Prior to immersion test, the substrate was abraded using emery paper up to 1200 grade, cleaned with acetone, etched in 10 % dilute sulphuric acid, washed with distilled water, and dried finally. The deposition rate was estimated from weight gain after 1 h of immersion time, assuming a Ni coatings density of 8.9 g cm⁻³ [15].

The morphology of the deposits was investigated by scanning electron microscopy, the composition estimated by EDX analysis and the crystalline structure by X-ray diffraction using a cobalt anticathode.

For the cyclic voltammetry measurements, a conventional three electrode cell was employed. It involved the use of glassy carbon samples as the working electrode, while the auxiliary electrode consisted of a Pt plate. All potentials were measured and reported with respect to saturated calomel electrode (SCE). The polarization curve was recorded by polarization from 1000 mV/SCE towards more negative direction (-1200 mV/SCE) with a sweep rate of 10 mV/s which the minimal value to observe the reaction occurred at the metallic surface. These measurements were carried out using Potentiostat/Galvanostat/Voltalab PGZ 100 monitored by a personal computer.

The electrochemical impedance spectroscopy measurements were carried out using a transfer function analyzer, over the frequency range from 100 kHz to 0.01 Hz with 10 points per decade. The applied amplitude of AC signal was 10 mV_{rms}. For all experiments were performed at the open circuit potential. The EIS diagrams were done in the Nyquist representation. The results were then analyzed in terms of an equivalent electrical circuit using Bouckamp program [16].

3. Results and discussion

3. 1. Influence of ammonium acetate on the deposition rate and phosphorus content

Figure1 presents the effect of ammonium acetate concentration on the deposition rate and the phosphorus content of Ni-P electroless deposition. Without ammonium acetate, the deposition rate is about $5 \mu\text{m h}^{-1}$. This deposition rate value is quite low for the industries applications.

When the ammonium acetate concentration increases from 0 to 32.5 g L^{-1} , the deposition rate increases rapidly from 5 to $18 \mu\text{m h}^{-1}$ while the phosphorus content decreases from 11 to 6.5 wt%. In addition, it is found that for the ammonium acetate concentration above 32.5 g L^{-1} , the bath decomposes spontaneously. In other studies [17], when an aqueous mixture of sodium acetate and nickel chloride (0.5 mol L^{-1}) was used, a spectroscopy analysis showed that the composition was as follows: bisacetato nickel complex $[\text{Ni}(\text{CH}_3\text{COO})_2]$ (2%), monoacetato nickel complex $[\text{Ni}(\text{CH}_3\text{COO})]^+$ (16%), $[\text{CH}_3\text{COO}]^-$ and $[\text{Ni}(\text{H}_2\text{O})_6]^{2+}$ (82%), suggesting that although nickel acetate is forming some complex in aqueous solution which it is still considerably dissociated. Again this would suggest that the role of acetic acid in EN solutions was unlikely to be that of a complexing agent, but it was rather a buffering agent. Besides, ammonium acetate has been used as complexing and stabilizing agent in Ni-P [18-20] and Ni-Cu-P [21-22] electroless plating baths. In alkaline Ni-P solutions, it was been shown that the solution stability was increased in the presence of ammonium acetate or ammonium chloride [20]. In acidic Ni-Cu-P solutions, when the copper sulfate concentration is increased from $4 \times 10^{-4} \text{ mol L}^{-1}$ to $8 \times 10^{-4} \text{ mol L}^{-1}$, in the absence of ammonium acetate, the solution decomposed spontaneously [22]. In addition, the copper content increased markedly from 1.5 wt % to 10 wt % due to the addition of ammonium acetate [22]. In our case, the increase of deposition rate and nickel content with the ammonium acetate addition could be due to two actions. Firstly, ammonium acetate could participate in the formation of the reactive intermediate and could facilitate the hypophosphite ion oxidation through adsorption on the catalytic metal surface. Secondly, NH_3 and $[\text{CH}_3\text{COO}]^-$ could form ions with low complexation contains with Ni^{2+} ions in solution, easily dissociated:

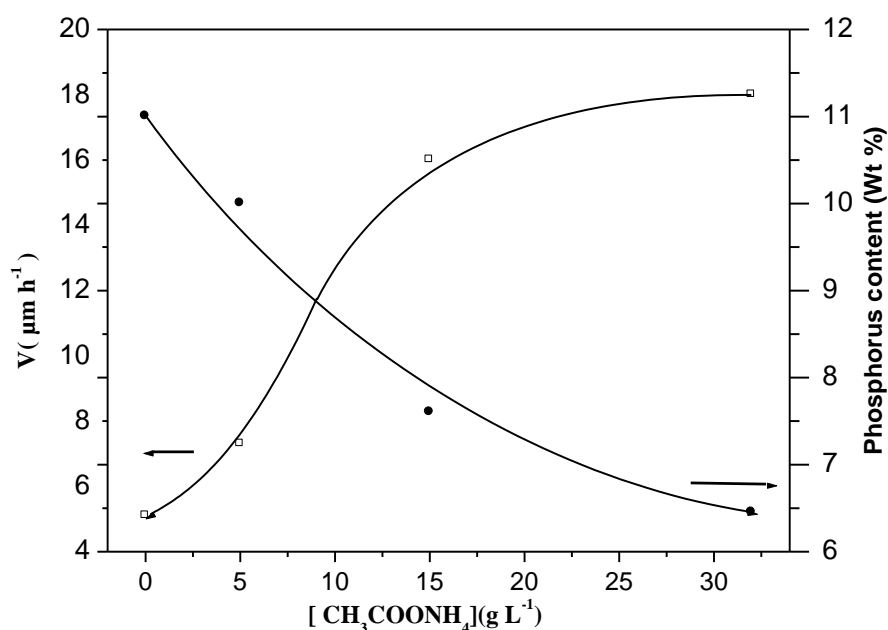


Figure 1: Effect of ammonium acetate concentration on deposition rate and phosphorus content of Ni-P electroless deposition

3. 2. Activation energy of Ni-P electroless deposition

Both chemical and electrochemical reactions depend on solution temperature. Figure 2 shows that the logarithm of the deposition rate increases quasi linearly with the reciprocal temperature without and with 32.5 g L⁻¹ of ammonium acetate (optimum values for the greater deposition rate). The activation energies values calculated without and with 32.5 g L⁻¹ of ammonium acetate are similar (about 31.3 kJ mol⁻¹ and 31.6 kJ mol⁻¹, respectively) indicating that the addition of ammonium acetate does not affect the activation energy. This result can be explained by the formation of the less stable reactive intermediate. In addition, these values may be compared with the values mentioned, for the oxidation of hypophosphite at pH 9, which lye in the range 33–88 kJ mol⁻¹ depending on the nature of the substrate (46 kJ mol⁻¹ on Ni) [22, 29].

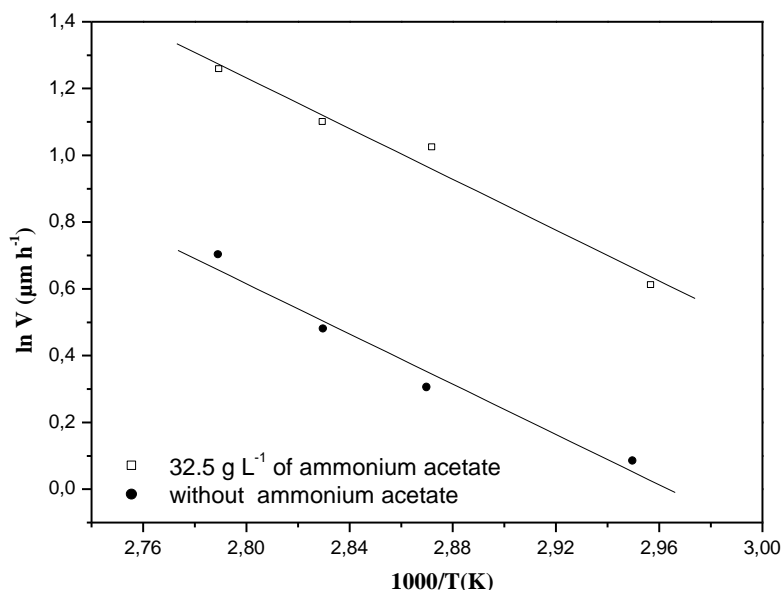


Figure 2: Arrhenius plot of deposition rate for Ni-P electroless deposition without and with 32.5 g L⁻¹ of ammonium acetate

3. 3. Morphology and structure of Ni-P electroless deposition

Figure 3 (a-d) shows the surface morphologies of Ni-P electroless deposition obtained at different ammonium acetate concentrations. For all coatings, a spherical nodular morphology can be observed even if the nodules size and density depend on ammonium acetate concentration. In addition, with 32.5 g L⁻¹ of ammonium acetate, the Ni-P deposit is more homogeneous and more compact. This can be mainly attributed to (i) the stability role of ammonium acetate which can stabilize the nucleation and growth of grains and (ii) the relationship between the grains size and the phosphorus content in the deposits as shown by Lu and Zangari [23] that indicated that the grain size of Ni-P coatings decreases with increasing phosphorus content in the deposits.

Figure 4 shows the XRD diffractions patterns of Ni-P electroless deposits obtained at various ammonium acetate concentrations. The X-ray diffraction patterns of electroless Ni-P coatings exhibit only a single broad peak at about 2θ = 42°. In the absence and the presence of 5 g L⁻¹ of ammonium acetate, the Ni-P deposits have an amorphous structure. It can be seen that, when the ammonium acetate concentration increases from 5 g L⁻¹ to 32.5 g L⁻¹, the peaks width decrease and the Ni-P deposit becomes crystalline with face centred cubic phase formation of Ni (111) preferred orientation [22]. This result can be explained by the decreasing from 11 to 6.5 wt % of the phosphorus content in the deposit. This is in agreement with the results showing that at lower P

contents the deposits were crystalline and when it is higher than 7 wt % [24] or 8 wt % [25] the deposits became amorphous.

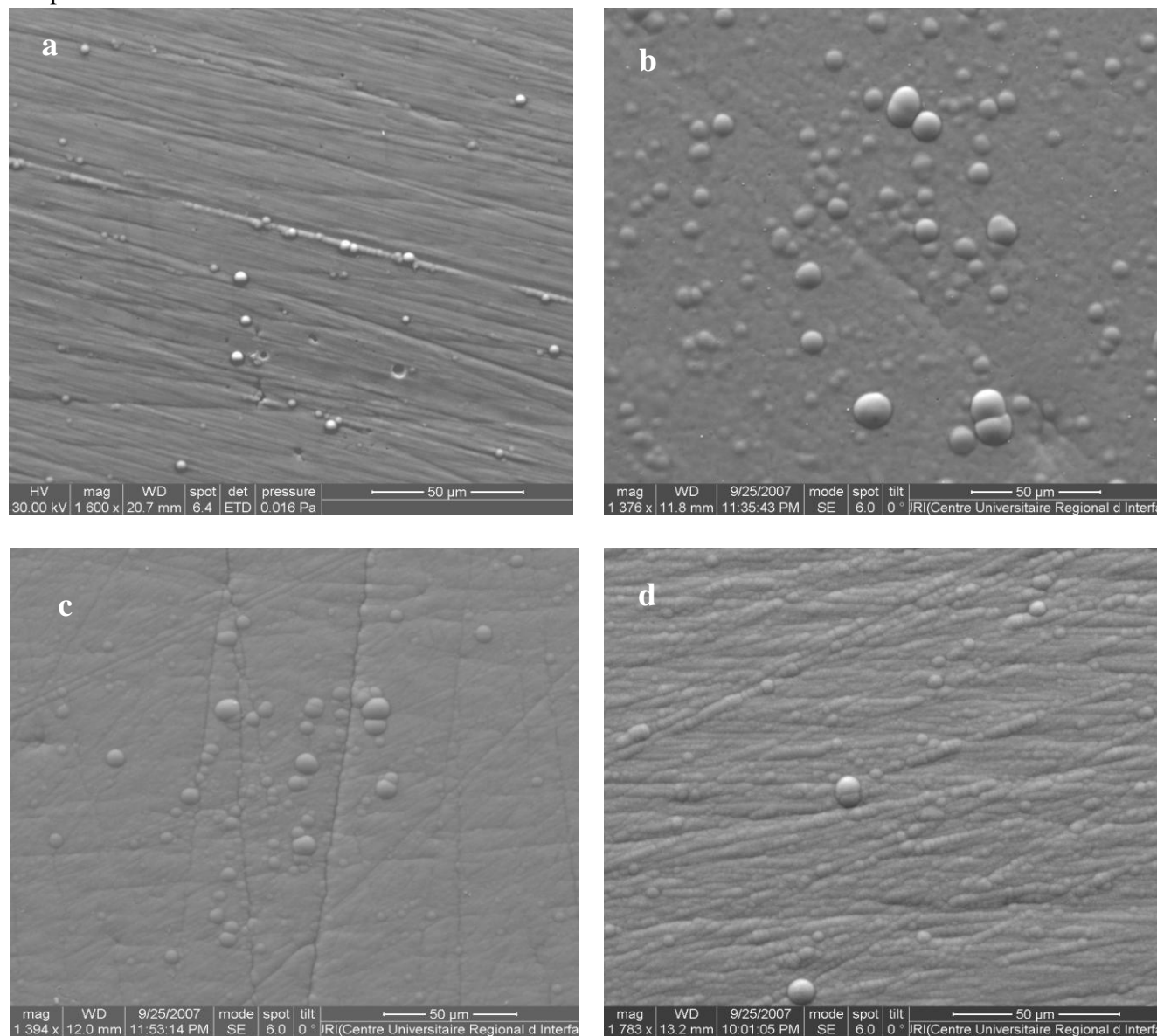


Figure 3: SEM micrographs of Ni-P electroless deposition obtained at different ammonium acetate concentration: (a) 0 g L^{-1} (11 % P); (b) 5 g L^{-1} (10 % P); (c) 15 g L^{-1} (7.5 % P); (d) 32.5 g L^{-1} (6.5 % P)

3.4. Kinetics studies

i. Cyclic voltammetry studies

The autocatalytic deposition of metal or alloy usually result is a consequence of a red-ox reactions. However, several interactions often occur between these reactions [26, 27]. For these, cyclic voltammetry was carried out to characterize the effect of ammonium acetate concentration on various red-ox processes. The obtained results are presented in Figure 5. The voltammograms reveal the existence of: (i) a cathodic peak K (at -1100 mV/SCE), attributed to the reduction reaction of Ni^{2+} , H_2PO_2^- and H_3O^+ ions; (ii) An anodic peak A located at -500 mV/SCE , relating to the oxidation of H_2PO_2^- ions and adsorbed hydrogen atoms at the metallic surface; (iii) An anodic peak B, at 250 mV/SCE in the absence and the presence of 5 g L^{-1} to 15 g L^{-1} of ammonium acetate and at

300 mV/SCE in the case of 32.5 g L⁻¹ was observed, this peak is related to the crystalline Ni-P deposit dissolution; (iv) the anodic peak C at 450 mV/SCE, in the absence and the presence of 5 g L⁻¹ to 32.5 g L⁻¹ of ammonium acetate was attributed to the amorphous Ni-P deposit dissolution. In addition, it is noted that these peaks were shifted to the anodic direction with the ammonium acetate concentration indicating the change of the nature and the thickness of the deposit surface.

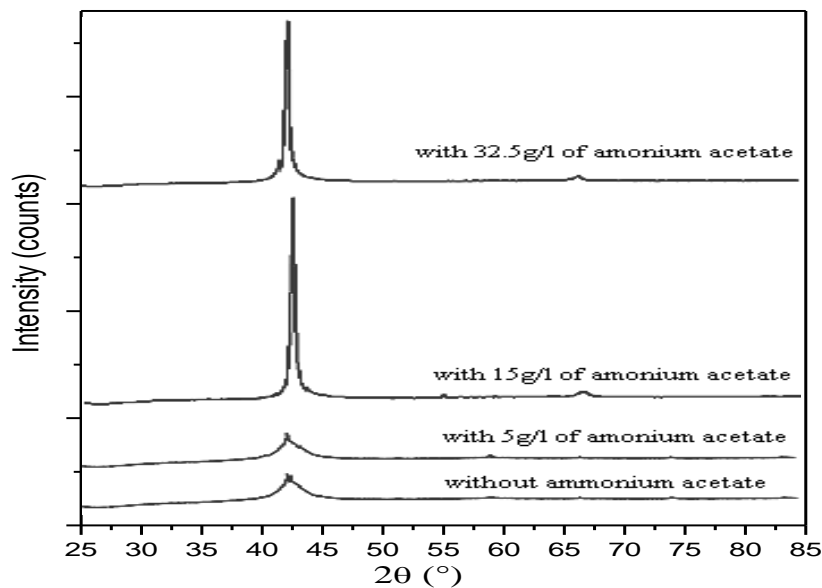


Figure 4 : XRD pattern electroless Ni-P deposit obtained at various ammonium acetate concentrations.

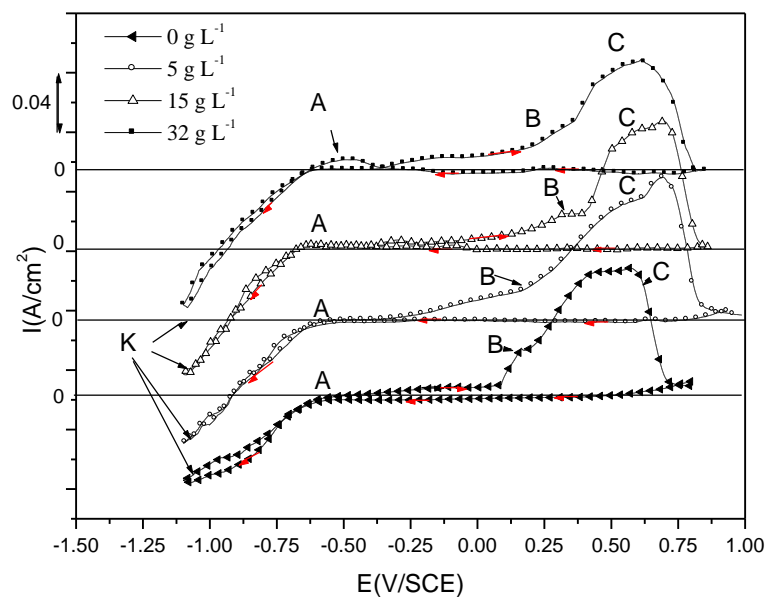
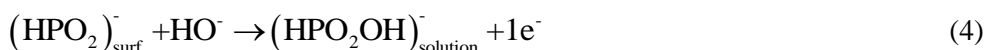


Figure 5: Voltammograms recorded on glassy carbon electrode of electroless Ni-P deposits at various ammonium acetate concentrations (Scan rate 10 mV s⁻¹).

Figure 6 shows the currents densities evolution of cathodic I_K and anodic I_A peaks versus ammonium acetate concentration. It is noted that the peaks intensities I_K and I_A increase with ammonium acetate concentration indicating that this compound acts in both fields: anodic and cathodic.

However, in our previous works, we studied the electroless Ni-P alloy in ammoniacal medium [19] and we showed that in anodic range, the chemical reaction was preceded by charge transfer reaction. This reaction was a deprotonation of hypophosphite ions which can be written as:



In addition, the anodic oxidation of hypophosphite is the dominant factor in electroless deposition [28, 29]. For this, we can propose that the ammonium acetate, by the means of its basic properties, enhances reaction (3) which supports the oxidation of hypophosphite. The enhancement of the anodic reaction favors the reduction of nickel ions which is the major reaction in the deposition process. So, the content of nickel in the deposit increases with ammonium acetate concentration.

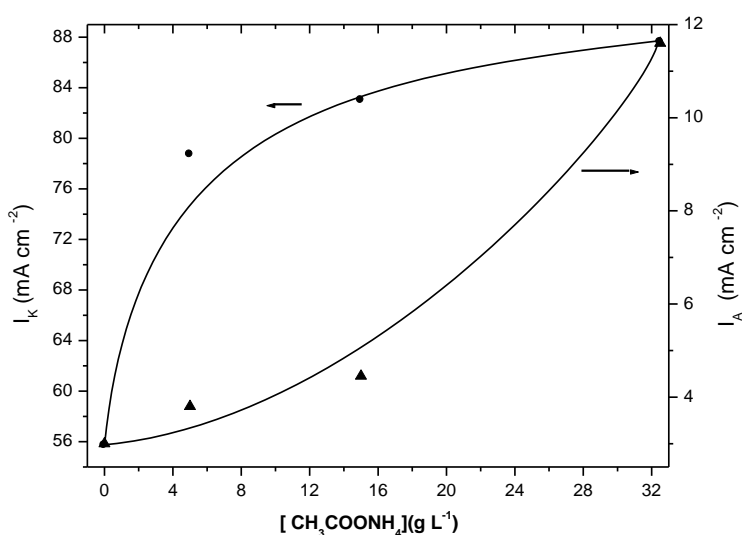


Figure 6: Currents densities evolution of cathodic I_K and anodic I_A peaks versus ammonium acetate concentration.

ii. Electrochemical impedance spectroscopy studies:

The deposition potential is characterized by a net current equal to 0, resulting from two simultaneous anodic (oxidation of hypophosphite) and cathodic processes (reduction of nickel ions, hypophosphite ions and hydrogen evolution). Figure 7 shows the impedance diagrams spectra obtained at plating potential for various ammonium acetate concentrations, an electrode rotation speed of 500 rpm.

In the absence of ammonium acetate, it can be obtained a characteristic impedance diagram of an electroless Ni-P alloy [26, 27]. This diagram presents:

- In the high frequency domain a capacitive loop appears which is related to the relaxation of the double layer capacitance C_{dl} in parallel with the charge transfer resistance R_t .

- A small inductive loop was observed with a characteristic frequency around a few Hz. Its size increases, for low hypophosphite or large nickel sulfate concentrations and without ammonium acetate. A similar inductive loop was observed in the case of electroless Ni-P deposition and it was attributed to the two-step discharge of the Ni^{2+} species through the intermediate NiI_{ads} adion [26, 27, 30-32]:



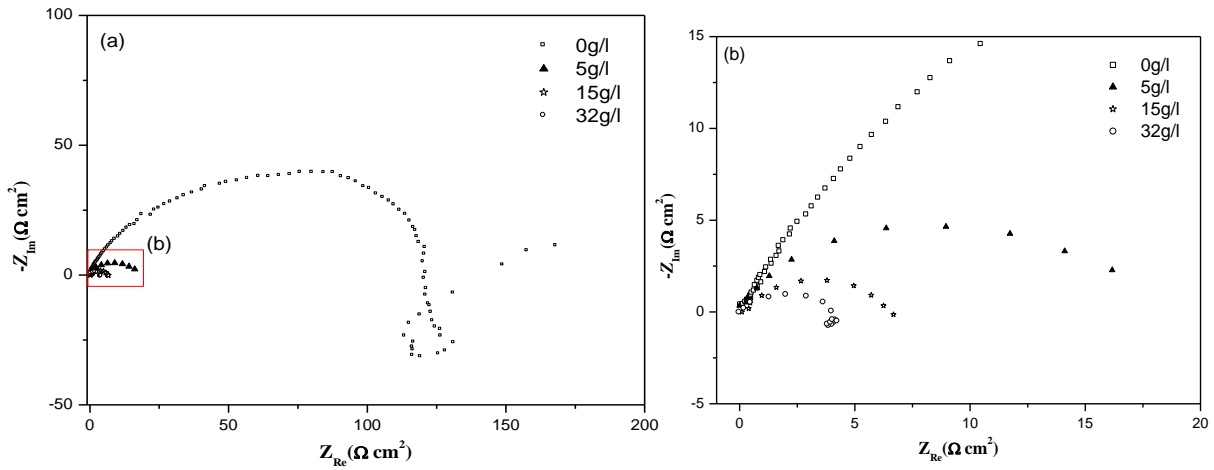


Figure 7: Impedance diagrams spectra recorded on glassy carbon electrode of electroless Ni-P deposits obtained at plating potential for various ammonium acetate concentrations ($\Omega = 500$ rpm) ((b): the zoom at high frequency) .

This loop is not observed in the presence of 5 g L^{-1} and 15 g L^{-1} of ammonium acetate, while it appeared in the case of 32.5 g L^{-1} .

At lower frequencies, a second capacitive loop was observed in the absence of ammonium acetate. Its size increases with pH, with hypophosphite concentration and with nickel sulfate concentrations [27]. A similar capacitive loop has been previously observed in the case nickel deposition in acidic solutions and it was attributed to interactions with adsorbed hydrogen, H_{ads} and nickel discharge [27, 31] according to:



The effect of ammonium acetate concentration on both the charge transfer resistance (R_t) and the double layer capacitance (C_{dl}) values are shown in Figure 8.

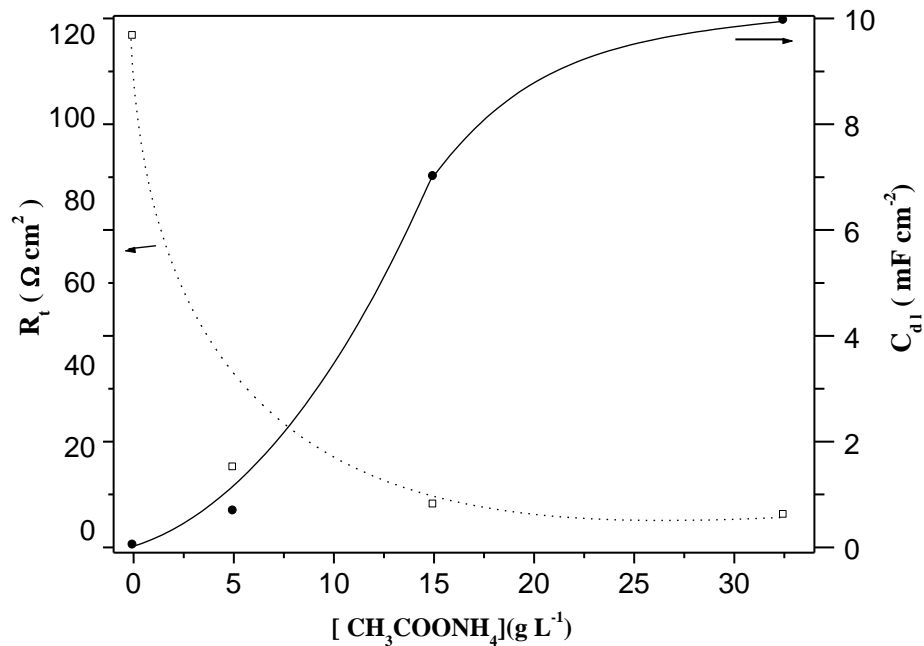


Figure 8 : Effect of ammonium acetate concentrations on the double layer capacitance C_{dl} and the charge transfer resistance (R_t)

The charge transfer resistance (R_t) values decreases rapidly from 120 to 4 $\Omega \cdot \text{cm}^2$ with increasing of ammonium acetate concentration from 0 to 32.5 g L^{-1} . This change confirms the accelerating effect of ammonium acetate, in agreement with the result obtained by gravimetric measurements. Also, the double layer capacitance (C_{dl}) values increases from 33 to 9952 $\mu\text{F cm}^{-2}$. This indicates that the ammonium acetate acts the surface roughness. Indeed, the high value of double layer capacitance ($C_{dl} = 9952 \mu\text{F cm}^{-2}$ at 32.5 g L^{-1} of ammonium acetate) may also indicate an increase of surface roughness.

Conclusion

The effect of ammonium acetate as additive on the formation and characteristics of electroless Ni-P deposits obtained from an acidic hypophosphite reduced electroless nickel bath was investigated. The study shows that the deposition rate of electroless Ni-P plating increases with increasing ammonium acetate concentration. In addition, when ammonium acetate concentration is above 32.5 g L^{-1} the bath spontaneously decomposes. It is also found that the ammonium acetate concentration influences the deposits composition and the structure, and also improves the morphology of deposits. Indeed, at 32.5 g L^{-1} of ammonium acetate, a spherical nodular structure becomes more homogeneous and more compact. The electrochemical investigations confirm the effect of ammonium acetate such as accelerator. Electrochemical measurements showed that the kinetic parameters depend on the ammonium acetate concentration. The electrochemical and gravimetric measurements were in good agreement.

5. References

1. Glenn O.M, American Electroplaters and Surface Finishers Society, Florida [AESF] 1992
2. Salvago G. and Cavallotti P.L, *Plating*, 57 (1972) 665
3. Van Den Meerakker J.E.A.M, *J. Appl. Electrochem.*, 11 (3) (1981) 395.
4. Schlesinger M., Paunovic M. (Eds.). *M. Modern Electroplating*, 4th ed., John Wiley & Sons, Inc., New York, 2000, Chapter 18.
5. Chen K. and Chen Y., *Plat. Surf. Finish.*, 84 (1997) 80.
6. Paunovic M. and Arndt R., *J. Electrochem. Soc.*, 130 (4), (1983) 794.
7. Ying H. G, Yan M, Ma T. Y, Wu J.M. and Yu L. Q, *Surface & Coatings Technology*, 202 (2007) 217-221.
8. Huang Y. S. and Cui F. Z, *Surface & Coatings Technology*. 201, (2007) 5416.
9. Lin K. L. and Hwang J. W, *Mater.Chem. Phys.* 76 (2002) 204.
10. De Minjer C. H. and Brenner A., US Patent. 2. 929, 1973) 742.
11. Keong K. G., Sha W. And Malinov S, *J. Alloys Compd.* 334 (2002) 192.
12. Ambat R. and Zhou W, *Surf. Coat.* 179, (2004) 124.
13. Baskaran I., Sankara Narayanan T.S.N and Stephen A, *Mater. Chem. Phys.*, 99 (2006) 117.
14. Namboodiri P. N. N, Prasad K. V and Mathur P. B., *Trans. SAEST*, 7 (1972) 122.
15. Møller P., Rasmussen J.B., Köhler S., Nielsen L.P., *NASF Surface Technology White Papers* 78 (3) (Dec 2013) 15-24
16. Bouckamp A., *Users Manual Equivalent Circuit*, Ver. 4.51, 1993
17. Rose S. J., Gustar R. E., Mihara D. R., Bickley R. I., Edwards H.G. M., Knowles A, *Inst. Metal Finish.* 73 (1) (1993) 11.
18. Cherkaoui M. and Chassaing E, *Inter finish*, 92 (1992) 127.
19. Ebn Touhami M., Cherkaoui M., Srhiri A., Bachir A. B., Chassaing. E, *J. Appl. Electrochem.* 26 (1996) 487.
20. Chassing E., Cherkaoui. M and Srhiri. A, *J. Appl. Electrochem.* 23 (1993) 1169.
21. Larhzil H., Cissé M., Tourir R., EbnTouhami M. and Cherkaoui M., *Electrochim. Acta*, 53 (2007) 622.
22. Tourir R., Larhzil H., EbnTouhami M., Cherkaoui M., Chassaing, *J. Appl. Electrochem.* 36 (2006) 69-75.
23. Lu G. and Zangari G, *Electrochim. Acta*, 47 (2002) 2969.
24. Mallory G.O. Haidu J.B eds, AESF Orlando (1990)
25. Mai Q. X., Daniels R. D. and Harpalani H. B. *Thin Solid Films.* 166 (1988) 235.
26. Ebn Touhami M., Chassaing E. and Cherkaoui M, *Electrochimica Acta*, 48 (2003) 3651.
27. Ebn Touhami M., Chassaing E. and Cherkaoui M, *Electrochim. Acta*, 43, (1998) 1721.
28. Ohno I., *Mater.Sci. Eng. A.* 146,1991,33.
29. Ohno I., Wakabayashi. O and Haruyama. S., *J. Electrochem. Soc.* 132, (1985) 2323.
30. Epelboin I., Jousselein M. and Wiart R, *J. Electroanal. Chem.* 119 (1981) 61.
31. Chassaing E., Jousselein M. and Wiart R., *J. Appl. Electrochem.* 157 (1983) 75.
32. Chassaing E., Vu Quang K. and Wiart R., *J. Appl. Electrochem.*, 17 (1987) 1267.